Carbohydrate Research, 215 (1991) 159–178
Elsevier Science Publishers B.V., Amsterdam

Optimization of waveforms for pulsed amperometric detection (p.a.d.) of carbohydrates following separation by liquid chromatography

William R. LaCourse and Dennis C. Johnson*
Department of Chemistry, Iowa State University, Ames, IA 50011 (U.S.A.)

(Received August 8, 1990; accepted in revised form November 28th, 1990)

ABSTRACT

Pulsed amperometric detection (p.a.d.) has recently gained prominence as a sensitive detection system for polar aliphatic organic compounds separated by liquid chromatography (l.c.). P.a.d. is based on the application of triple-step potential waveforms to incorporate amperometric detection with alternated anodic and cathodic polarizations to clean and reactivate electrode surfaces. These polarization steps result in the maintenance of uniform electrode activity for detection of organic compounds that typically are observed to "foul" noble metal electrodes during extended periods of amperometric detection at constant (dc) applied potential. Carbohydrates are easily separated with anion-exchange chromatography using alkaline mobile phases, and these alkaline conditions are appropriate for the direct detection of all carbohydrates at Au electrodes by p.a.d. The voltammetric and chronoamperometric responses are described here for selected carbohydrates, and guidelines are given for selection of optimal potential and time parameters in the waveform to be used for l.c.–p.a.d..

INTRODUCTION

Pulsed amperometric detection (p.a.d.) has gained prominence over the last decade as a sensitive detection system for sugar alcohols, monosaccharides, and oligosaccharides following their separation by liquid chromatography (l.c.)[1]. Detected also are amino alcohols, amino glycosides, amino acids, and some sulfur compounds. Most frequently, p.a.d. is applied at Au electrodes under alkaline conditions (pH >12) in miniature flow-through electrolysis cells[2]. The advance of robust, alkali-tolerant, polymer-based, ion-exchange phases has complemented p.a.d., and carbohydrates are now easily separated by anion-exchange chromatography using alkaline mobile phases[3]. Sensitivity for monosaccharides in l.c.–p.a.d. is comparable for aldoses and ketoses with detection limits of ~ 1–10 pmoles. The sensitivity of p.a.d. for simple alcohols is better at Pt than at Au electrodes, with acceptable detectability even under acidic conditons. A review of l.c.–p.a.d. has recently been published[4].

The significance of p.a.d. within chemical and biochemical analysis can be best appreciated in view of the commonly held impression, based on attempted detections at constant (dc) applied potential, that aliphatic compounds are generally not electroac-

* To whom correspondence should be addressed.

0008-6215/91/$ 03.50

TABLE I

(A) General and (B) optimal waveform parameters for pulsed amperometric detection (p.a.d.) at an Au working electrode in 0.1M NaOH

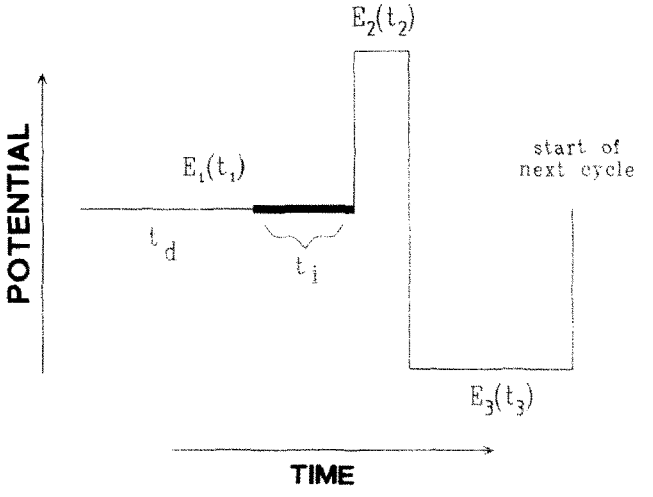

A

Potential (*mV* vs. *Ag/AgCl*)	*Time* (*ms*)	*Function*
E_1, −250– +250	t_1, >120	detection
	t_d, >100	delay
	t_i, > 20	signal sampling
E_2, +600– +800	t_2, > 60	oxidative cleaning
E_3, −800– −200	t_3, >120	reductive reactivation and adsorption of analyte

B

Potential (*mV* vs. *Ag/AgCl*)			*Time* (*ms*)		
	PAD	*PED*		*PAD*	*PED*
E_1,	+150	+150	t_1,	720	1460
			t_d,	520	860
			t_i,	200	600
E_2,	+700	+700	t_2,	120	120
E_3,	−300	−300	t_3,	360	360

tive. Furthermore, aliphatic compounds do not possess chromophoric or fluorophoric groups, and, hence, direct and sensitive detection by photometric techniques is not possible. Conversely numerous aromatic compound (*e.g.*, phenols, aminophenols, catecholamines, and other metabolic amines) are detected very easily by anodic reactions at a constant (dc) applied potential at inert electrodes, including those of Au, Pt, and carbon[5]. Thus, a brief consideration of the difference in reactivities is appropriate.

Electronic resonance in aromatic, conjugated molecules can function to stabilize free-radical intermediate products of anodic oxidations, and, as a consequence, the activation barrier for electrochemical reaction is significantly lowered. In contrast, absence of π-resonance stabilization in aliphatic compounds results in very low oxidation rates, even though the reactions may be thermodynamically favored[6]. Alternately, stabilization of free-radical products can be achieved *via* adsorption to the surface of noble metal electrodes which have empty *d*-orbitals. Unfortunately, adsorption of organic molecules and free radicals frequently has the consequence of fouling of the electrode and loss of reactivity[7]. Hence, observations of non-reactivity for aliphatic compounds at noble metal electrodes can be attributed commonly to surface fouling as a result of high but transient catalytic activity.

The technique of p.a.d. utilizes triple-step potential-time (E–t) waveforms which incorporate the processes of amperometric detection with alternated anodic and cathodic polarizations to clean and reactivate the electrode surface (see Table I). The detection potential (E_1) in the waveform is chosen to be appropriate for the desired surface-catalyzed reaction, and the electrode current is sampled during a short time

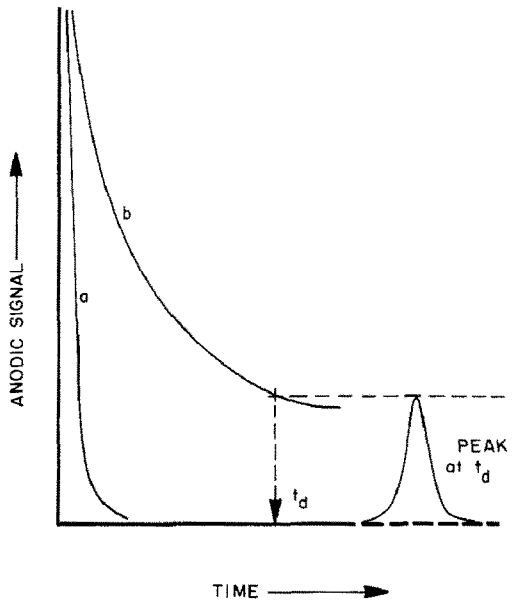

Fig. 1. Chronoamperometric response (i–t) following a potential step from E_3 to E_1 in the p.a.d. waveform (a) without and (b) with analyte present to illustrate the origins of chromatographic baseline and peak signals in l.c.–p.a.d.. The delay prior to current sampling is denoted by t_d.

period (t_3) after a delay of t_d near the end of the detection period (t_1). Following the detection process, adsorbed carbonaceous species (*e.g.*, free radicals) are oxidatively desorbed by an electrocatalytic process occurring simultaneously with anodic formation of surface oxide following a positive step to the value E_2 (t_2). The activity of the "clean" electrode surface is then regenerated by a subsequent negative potential step to E_3 (t_3) to achieve cathodic dissolution of the oxide film prior to the next cycle of the waveform. The use of on-line, pulsed cleaning, and reactivation of noble metal electrodes is sufficient to maintain reproducibly high electrode activity. Although pulsed waveforms have been applied to carbon electrodes[8,9], those electrodes have not generally been successful for aliphatic compounds.

Anodic detection of the aldehyde and alcohol functionalities in carbohydrates occurs in a potential region where there is only a very small signal for the concurrent formation of surface oxide. Direct detection on oxide-free surfaces is designated as "Mode I". The experimental basis of detection peaks for carbohydrates by Mode I in l.c.–p.a.d. is illustrated in Fig. 1 by the chronoamperometric (i–t) response curves generated following the potential step E_2 to E_1 in the p.a.d. waveform. The residual current (curve *a*) decays quickly, and the baseline signal in l.c.–p.a.d. is minimal for $t_d > \sim 100$ ms. Curve b in Fig. 1 represents the transient i–t response for the presence of the reactant and the peak shown is representative of the corresponding signal expected in l.c.–p.a.d. for the value of t_d indicated. Mode II corresponds to detections catalyzed by simultaneous formation of surface oxide, and is especially useful for amines, amino acids, and sulfur compounds.

Recently, Andrews and King[10] have described a method for optimizing pulse potentials for p.a.d. using voltammetry. Although the selection of potentials was investigated, the strategy for optimizing timing parameters of the potential-time waveforms was completely ignored. In contrast, described herein are voltammetric and chronoamperometric response characteristics for several carbohydrates at Au electrodes in alkaline media. Guidelines are also presented for the optimization of all parameters of the p.a.d. waveform.

EXPERIMENTAL SECTION

Carbohydrates and other reagents. — All solutions were prepared from reagent-grade chemicals. Triply-distilled water was further purified in a Millipore Milli-Q™ system (Millipore Corp., Bedford, MA). Mobile phases containing NaOH were diluted from a 50% (w/w) NaOH stock solution. Acetonitrile was h.p.l.c. grade (Fisher Scientific, Springfield, NJ). All mobile phases were filtered before use with 0.45-μm Nylon-66 filters (Rainin Corp., Woburn, MA) and a solvent filtration kit. Solutions for voltammetric studies were deaerated to remove dissolved O_2 by dispersion of N_2.

Apparatus. — Voltammetric data were obtained at an Au (~ 0.2 cm^2) rotated disk electrode (Pine Instrument Co., Grove City, PA) with a RDE4 potentiostat (Pine). Current–time plots (i–t) were obtained by a DAS-16F high-speed A/D expansion board (MetraByte Corp., Taunton, MA), IBM™-AT-compatible computer, and SNAPSHOT Storage Scope software (HEM Data Corp., Southfield, MI).

Separations were performed using a CarboPac-PA1 separator column (Dionex Corp., Sunnyvale, CA) in an isocratic–gradient chromatography system (Dionex). Post-column addition of reagent was by a Reagent Delivery Module (RDM, Dionex). A 375-μL woven reactor was placed after the "mixing-tee' to mix the reagent and eluant streams. Injection volumes were 25-μL.

Pulsed detection was performed with a Model PED (Dionex) at an Au working electrode with an Ag/AgCl reference electrode. The method of current sampling in PED is by digital integration, and, therefore, signal output is electronic charge (q) with units of coulombs (coul.). Signal output in p.a.d. is electrode current (i) with units of coul. s^{-1}. Interconversion of units can be made *via* $i = q/t_i$, where t_i is the period of signal integration. Data were collected with an IBM™-AT-compatible computer with an Advanced Computer Interface (Dionex) and AI-450 software.

Procedures. — Potential–time waveforms used to obtain the p.a.d. data presented here were simulated using a programmable PED system (Dionex). This strategy allowed for an in-depth study of many of the parameters inherent to p.a.d. However, it is important to note, that the analog circuitry of a PAD (Dionex) unit is less noisy than the digital circuitry of a PED unit. Thus, application of the principles presented in this paper will be equivalent or better using PAD instrumentation. The PAD unit is limited in selectability of all time parameters.

All electrochemical reactions occur as a sequence of finite steps. Hence, if the rate of one particular step is significantly slower than all other steps, the electrode current is limited by the slow step in the reaction mechanism. In the simplest imaginable case, the sequence of steps in an electrochemical reaction includes (*i*) the convective–diffusional transport of reactant from the solution of the electrode surface, (*ii*) dissociative and/or other chemical processes which accompany conversion of the reactant species into the appropriate activated state, and (*iii*) the actual transfer of electronic charge across the electrode–solution interface. Furthermore, as in the reactions of aliphatic compounds at noble metal electrodes, the nature of the electrode can be very influential by way of adsorptive interactions with the reactant (or reaction product). It is important, in the development of amperometric and voltammetric sensors, to characterize the electrode reaction as to the nature of the rate-controlling process. This is necessary to interpret sensor response to changes in operating conditions and concentration of reactant.

The development of p.a.d. in our laboratory usually begins with an examination of voltammetric response at rotated disk electrodes (r.d.e.s) in large electrolysis cells. The current (i) produced at the r.d.e. is described by the Koutecky–Levich equation[11] (eq. *1*) given below.

$$i = \frac{nFADC^b}{1.61D^{1/3}v^{1/6}w^{-1/2} + D/k_{app.}} \qquad (1)$$

In Eq. *1*: n is the number of electrons (equiv. mol^{-1}), F is the Faraday constant (96 486.6 coul. $equiv^{-1}$), A is the geometric surface area of electrode (cm^2), D is the diffusion coefficient of reactant (cm^2. s^{-1}), w is the electrode rotational velocity (rad. s^{-1}), v is the

kinematic viscosity of solution ($cm^2\ s^{-1}$), C^b is the bulk concentration of reactant (mol. cm^{-3}), $k_{app.}$ is the apparent rate constant of the heterogeneous reaction ($cm\ s^{-1}$). If $k_{app.} >> 0$, *i.e.*, $D/k_{app.} \rightarrow 0$, the electrode response is under *transport* control, and an $i\text{-}w^{1/2}$ plot is linear with a zero intercept. Negative deviation from a linear $i\text{-}w^{1/2}$ plot, usually for large w values, indicates a finite value for $k_{app.}$. Such a condition is described as corresponding to *mixed* control. For small values of $k_{app.}$, the term $D/k_{app.}$ dominates the denominator in Eq. *1*, and the current response is independent of w, as given by Eq. *2*. The effect of variation of rotation speed for the r.d.e. is similar to variation of flow rate in an l.c. system with electrochemical detection in that changes in rotation speed and flow rate alter the linear velocity of fluid passing over the electrode surface which, in turn, controls the thickness of the diffusion layer.

$$i = nFAk_{app.}C^b \qquad (2)$$

Generally, the effect of variation of potential scan rate (φ) is also determined for the voltammetric data (i–E). A linear $i\text{–}\varphi$ response usually indicates contribution of *surface*-controlled processes corresponding to a Faradaic reaction of the electrode surface and/or reaction of species accumulated on the electrode surface at potential values when no reaction occurred.

RESULTS AND DISCUSSION

Voltammetry. — The current–potential (i–E) response is shown in Fig. 2 for an Au r.d.e. in 0.1M NaOH with (----) and without (——) D-glucose in the absence of dissolved O_2. The residual response for the supporting electrolyte (——) exhibits anodic waves on the positive scan in the regions of $\sim +0.2$ to $+0.7$ V (wave A) for oxide formation and $E > +0.7$ V (wave B) for O_2 evolution. A cathodic peak obtained on the negative scan in the region of $\sim +0.3$ to -0.1 V (wave C) corresponds to the dissolution of the oxide formed on the positive scan. When dissolved O_2 is present, the cathodic reduction of O_2 (....) occurs in the region of ~ -0.1 to -0.8 V (wave D) for both the positive and negative scans.

With the presence of D-glucose (----), a reducing sugar, an anodic wave is observed on the positive scan beginning at ~ -0.6 V (wave E). This wave corresponds to oxidation of the aldehyde group to the carboxylate anion in this alkaline media[12]. A much larger anodic signal is obtained for the combined oxidations of the alcohol and aldehyde groups in the region of ~ -0.3 to $+0.4$ V (wave F). The anodic signal is attenuated abruptly during the positive scan with onset of oxide formation (wave A). The signal for $\sim +0.4$ to $+0.6$ V (wave G) in addition to that for oxide formation results from the anodic desorption of adsorbed D-glucose and/or intermediate products simultaneously with the formation of surface oxide on the Au electrode. The absence of signal on the negative scan in the region of $\sim +0.8$ to $+0.2$ V indicates the absence of activity for the oxide-covered electrode surface. Following cathodic dissolution of the oxide on the negative scan to produce wave C, the surface reactivity for D-glucose

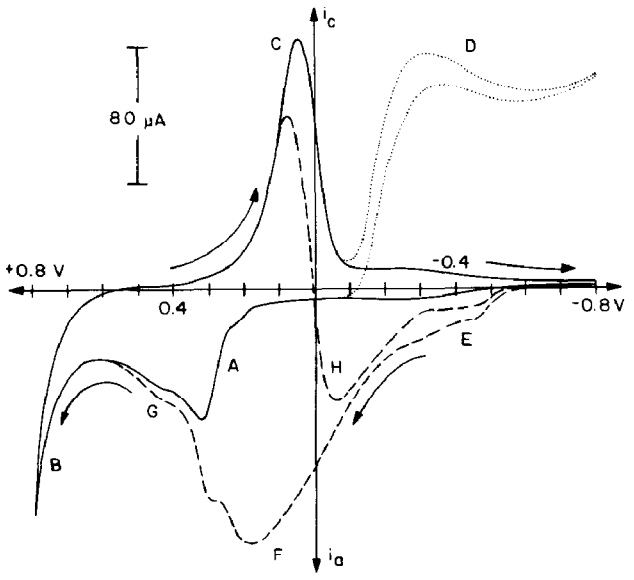

Fig. 2. Voltammetric response (i–E) for D-glucose at an Au r.d.e. Conditions: Rotation speed, 1000 rev. min^{-1}; scan rate, 200 mV s^{-1}; and Ag/AgCl reference electrode. Solutions: (·····) 0.1M NaOH with dissolved O_2; (——) 0.1M NaOH, deaerated; and (-----) 0.2mM D-glucose, deaerated.

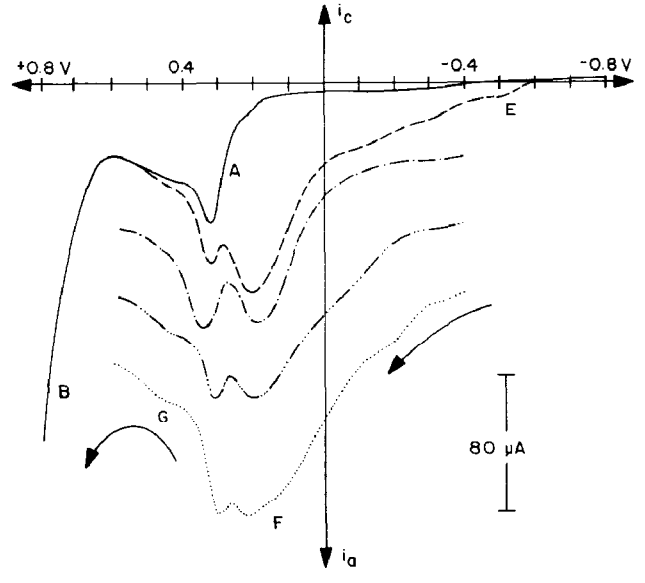

Fig. 3. Voltammetric response (i–E) for four carbohydrates in deaerated 0.1M NaOH. Positive scans from −0.8 to 0.8 V and currents greater than the background residual are shown. Each scan has been offset as indicated. Conditions: See caption to Fig. 2. Curves: (——) Residual; (·····) 0.15mM D-glucitol, offset: 120 μA; (–··–) 0.15mM D-fructose, offset; 80 μA; (—·—) 0.15mM sucrose, offset; 40 μA; and (-----) 0.15mM maltose, offset: 0 μA.

oxidation is immediately returned and an anodic peak (H) is observed for oxidation of alcohol and aldehyde groups on D-glucose. Anodic waves E, F, G, and H are all observed to increase in signal intensity with increases in D-glucose concentration.

Fig. 3 shows the i-E response obtained for the positive potential scans (*i.e.*, −0.8 to 0.8 V) at an Au r.d.e in 0.1M NaOH for representative carbohydrates at equimolar concentrations. Each scan is offset, and only currents greater than the background residual are shown. The carbohydrates shown include the following: D-glucitol, a reducing sugar alcohol (·····); D-fructose, a reducing ketose (– · –); sucrose, a non-reducing disaccharide composed of a D-glucose and a D-fructose bonded with an acetal–ketal linkage (– · –); and maltose, a reducing disaccharide composed of two D-glucose units bonded together with an acetal–acetal linkage (——). As indicated in Fig. 3, all of the carbohydrates show anodic signals corresponding to waves F and G for D-glucose (see Fig. 2). As with D-glucose, maltose produces an anodic wave (E) at ~ −0.6 V corresponding to aldehyde oxidation. This is expected since maltose and D-glucose are both reducing sugars.

The i–E curves in Fig. 3 indicate that analogous electrode processes are involved in the oxidations of the compounds selected. Hence, a single p.a.d. waveform can be designed to serve for detection of all carbohydrates under alkaline conditions. However, results obtained for variation of rotation velocity and potential scan rate indicate significant differences in reaction dynamics. The net maximum anodic current in wave F for D-glucose (Fig. 2) increases linearly as a function of the square root of rotation speed, as shown in Fig. 4 (-○-○-○-). Furthermore, there is no dependence on scan rate for D-glucose. These two observations support the conclusion that the mechanism producing wave F for D-glucose is primarily under transport control. The response of D-glucitol is similar to that of D-glucose and the same conclusion is valid. In contrast, wave F of

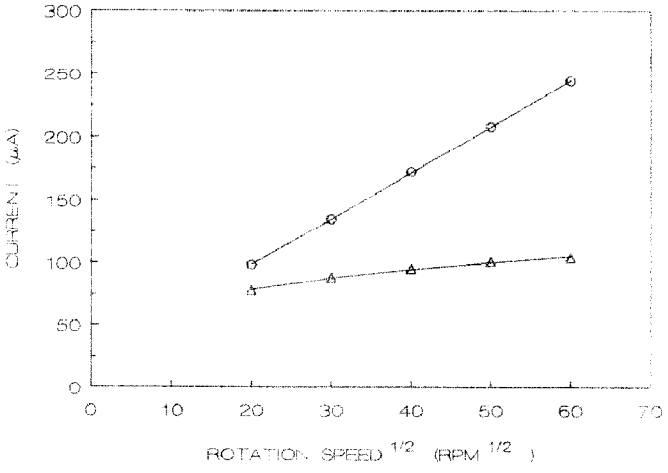

Fig. 4. Peak current response (i) as a function of the square root of rotation speed ($\omega^{1/2}$, rev. min^{-1}) at an Au r.d.e. in 0.1M NaOH. Conditions: Scan rate; 200 mV s^{-1} and Ag/AgCl reference electrode. Solutions: (○) 0.2mM D-glucose, (△) 0.2mM sucrose.

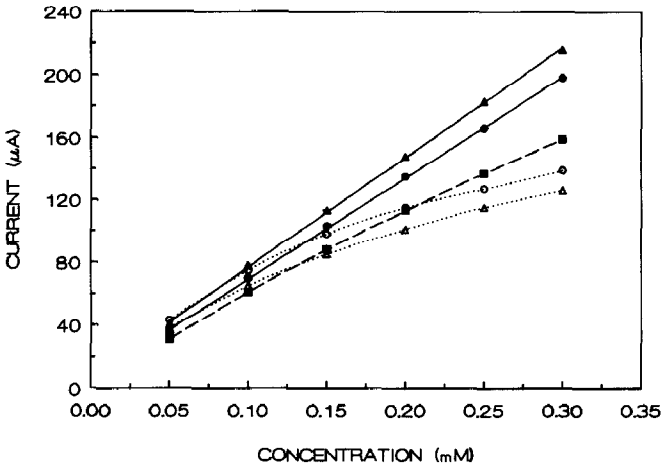

Fig. 5. Maximum current response (i) as a function of concentration for (▲) D-glucitol, (●) D-glucose, (■) D-fructose, (○) sucrose, and (△) maltose. Conditions: See caption to Fig. 2.

sucrose (see Fig. 3) increases with increasing scan rate, yet shows negligible change as a result of variations in rotation velocity, as shown in Fig. 4 (-△-△-△-). These observations indicate that wave F for the alcohol groups is under surface control. Maltose behaves similarly to sucrose. Fructose is under mixed control. It is important to note that the effects described are experimental classifications of the response denoted as wave F of each carbohydrate tested, and these results should not be extrapolated to infer that the groups of the carbohydrate with which the response is associated is responsible for its mechanism of detection.

One ramification of the differences in controlling mechanism for carbohydrate response is reflected in the shape of i–C^b plots. Carbohydrates which undergo transport-controlled reactions produce linear plots over larger ranges of C^b than for those reactions under surface control. Calibration data are shown in Fig. 5 for five carbohydrates studied at the Au r.d.e. in 0.1 M NaOH. As expected, the plots for D-glucitol (▲) and D-glucose (●) are more linear than those for sucrose (○) and maltose (△). The response of fructose is intermediate to those of D-glucose and sucrose. Two tentative explanations are offered for the nonlinear i–C^b plots for reactions characterized as being under surface control. First, the reactant molecules can be strongly adsorbed, and, therefore, response is controlled by the adsorption isotherm for that reactant. Second, if detection products are strongly adsorbed with the result of surface fouling, the current response will be attenuated more abruptly during the positive scan for large values of C^b for which full coverage of the surface is achieved more quickly.

All voltammetric data shown correspond to O_2-free solutions to emphasize carbohydrate response. Without deaeration, reduction of dissolved O_2 produces a cathodic wave at $E < -0.2$ V (see Fig. 2, curve D) which is well-resolved from the anodic wave for onset of Au oxide formation (see Fig. 2, wave A). This aspect of Au

TABLE II

Linearity of D-glucose response as a function of NaOH concentration[a]

NaOH (M)	*Linear range (pmole)*	*Slope (ncoul./pmole)*	*Intercept (ncoul.)*	R^{2b}
0.02	10–10 000	0.0958	−2.997	0.9999
0.05	10–10 000	0.1638	+0.367	1.0000
0.10	10–10 000	0.2456	+1.379	1.0000
0.20	10–10 000	0.3258	−9.377	0.9999

[a] D-Glucose response = ncoul. = slope(pmoles) + intercept. [b] R^2 = coefficient of correlation.

electrodes is in direct contrast to Pt electrodes where the cathodic wave for O_2 overlaps the anodic wave for Pt oxide formation[13]. Thus, Au electrodes are highly amenable to pulsed amperometric detection of carbohydrates in the presence of dissolved O_2. Uniformly low levels of dissolved O_2 are difficult to maintain in l.c. systems and choice of E_1 = 0.0–0.2 V for the p.a.d. waveform is a reasonable first estimate for universal carbohydrate detection without interference from O_2.

Selection of waveform parameters. — The selection of potential values for the p.a.d. waveform in l.c.–p.a.d. is readily discerned from the voltammetric (i–E) response obtained for the analyte(s) of interest. Table I describes (A) the acceptable ranges of p.a.d. parameters, as well as (B) the optimized values, for the triple-step waveform shown for p.a.d. of D-glucose at Au in 0.1M NaOH. Table IB lists of optimized parameters for p.a.d. at PAD and programmable PED units. It is evident from Fig. 2 that satisfactory results will be obtained for a rather wide range of E_1 values. However, the largest sensitivity for D-glucose at Au in 0.1M NaOH is obtained for E_1 = +150 mV. For this value, there exists only a very small contribution from surface oxide formation and virtually no contribution from reduction of dissolved O_2. As stated earlier, all carbohydrates exhibit a peak-shaped anodic response similar to that for D-glucose in Fig. 3 and, therefore, E_1 = +150 mV allows for universal detection of carbohydrates.

The choice of optimal timing parameters for the detection period in the p.a.d. waveform is not obvious from a review of the voltammetric response, and more information is required of the response dynamics in p.a.d. The chronoamperometric (i–t) response is shown in Fig. 6 following the step from E_1 to E_2. The residual response (curve A) corresponds to charging of the interfacial double-layer* and formation of a very small amount of surface oxide. This residual response decays very rapidly, and the baseline signal in l.c.–p.a.d. is very small for values of delay time (t_d) $\geq$ 100 ms. Curves B and C in Fig. 6 show the i–t responses obtained for the presence of D-glucose and

* A charged surface in contact with an electrolyte solution is counter-balanced by attracting ions of opposite charge and repelling ions of like charge. Two parallel layers of charge are formed: (i) the charge on the surface and (ii) the solution layer of oppositely charged ions near the surface. This structure is called the "interfacial double-layer"

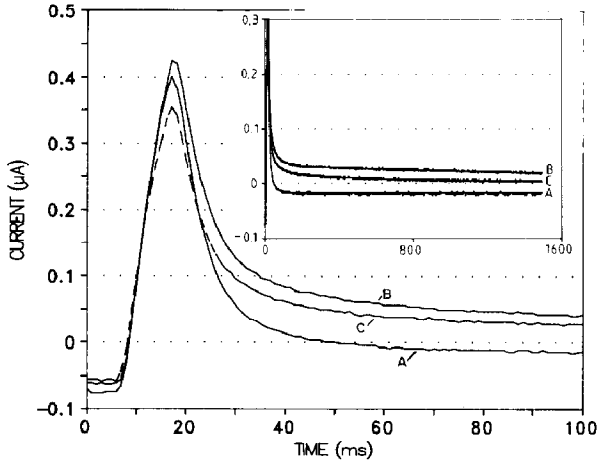

Fig. 6. Chronoamperometric response (i–t) for carbohydrates at the Au electrode in the l.c.–p.a.d. cell following the potential step from −300 mV (E_3) to 150 mV (E_1) in the p.a.d. waveform. Curves: (A) Residual, (B) 1mM D-glucose, and (C) 1mM sucrose. Conditions: Column, CarboPac-PA1; mobile phase, 0.1M NaOH; flow rate, 1.0 mL min^{-1}; injection volume, 25-μL; and p.a.d. waveform, see Table IB (PED).

sucrose, respectively. For any value $t_d > \sim 100$ ms (Fig. 6, insert), the anodic responses for both D-glucose and sucrose reach a pseudo steady-state value and positive (*i.e.*, anodic) peaks are obtained in l.c.–p.a.d. For values of t_d in the range 260 to 1260 ms, the l.c.–p.a.d. signal for 4μM samples of the carbohydrates tested (*i.e.*, 100 pmol per 25-μL injection) exhibit no evidence of current decay. This observation infers that minimal electrode "fouling" occurs for carbohydrates detected at low concentrations over the lifetime of the p.a.d. waveform. In fact, baseline drift and instability is diminished perceptibly with longer delay times, and an optimal value of $t_d = 860$ ms is chosen. Since the PAD unit is limited for selectable time parameters, the maximum t_i setting of 720 ms (Table IB) is chosen in order to have a t_d value of maximal duration.

It is interesting to note for $t_d < \sim 25$ ms in Fig. 6, that the signal for sucrose is slightly smaller than the residual current, and, as a consequence, negative peaks would result for sucrose. This effect for sucrose is believed to be related to the fact that a significant amount of sucrose is adsorbed at E_3. Adsorbed molecules cause a significant decrease in interfacial capacitance, with the result of a smaller signal for double-layer charging, as well as a suppressed rate of formation of the small amount of surface oxide normally formed at $E_1 = +150$ mV. Hence, for very small t_d, the total signal in the presence of sucrose is slightly smaller than the residual signal in the absence of sucrose.

Fig. 7 shows chromatograms for the separation and detection of five sugars using t_i values of 20 ms (curve A), 200 ms (curve B), and 800 ms (curve C). The signal-to-noise ratios (S:N) for D-fructose (c) in curves A, B, and C are 16, 87, and 97, respectively. The value of S:N reaches a nearly constant value for $t_i > \sim 500$ ms and, on this basis, an optimal value of $t_i = 600$ ms is chosen. For the PAD unit, the maximum t_i of 200 ms is chosen. These values of t_i are appropriate for all carbohydrates. It should be noted that 600 and 200 ms are multiples of 16.667 ms (1/60 Hz^{-1}), which aids in minimizing the noise originating from 60-Hz power sources.

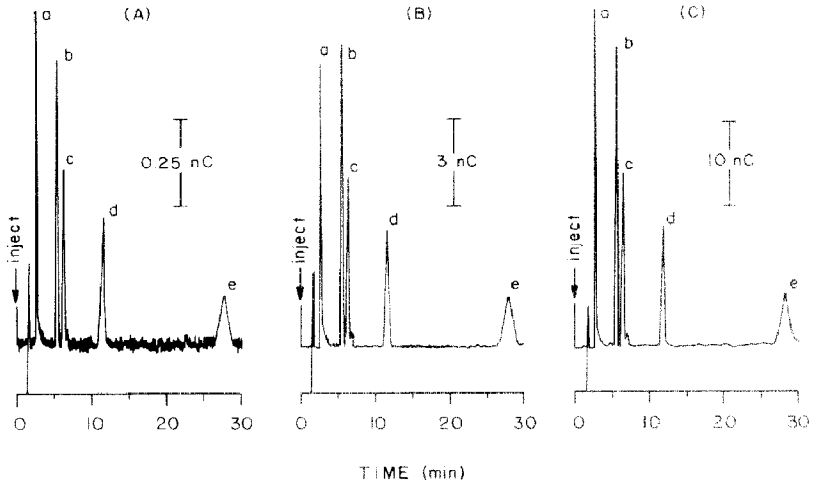

Fig. 7. Comparison of l.c.–p.a.d. results with variation of the integration time (t_1) in the p.a.d. waveform. Conditions: See caption to Fig. 6. Curves: (A) 20 ms, (B) 200 ms, and (C) 800 ms. Peaks (100 pmol each): (a) D-glucitol, (b) D-glucose, (c) D-fructose, (d) sucrose, and (e) maltose.

The anodic response for carbohydrates at a constant (dc) applied potential is attenuated as the electrode surface becomes fouled by the accumulation of adsorbed detection products. The strength of adsorption and rate of fouling vary with the identity of the reactant, and, generally, fouling for oligosaccharides is more severe than for monosaccharide (data not shown). Electrode activity is quickly regained in the p.a.d. waveform by oxidative desorption of the adsorbed species simultaneously with the formation of surface oxide ($E_2 = \sim +400$ to $+600$ mV), followed by cathodic dissolution of the oxide ($E_3 << -100$ mV). Current–potential curves are shown in Fig. 8A to illustrate the potential dependency of the oxidative cleaning processes. The oxidative removal of adsorbed residue from detection of sucrose and D-fructose are designated as waves G. Note that the small wave G for sucrose (···) is larger in area and located at a slightly more positive potential than that for D-fructose (——). This trend continues as the number of carbohydrate units is increased in the polysaccharide (data not shown). Thus, the more strongly adsorbed oligosaccharides and their detection products require larger E_2 values. Recent results indicate that some oxidative cleaning reactions occur simultaneously with O_2 evolution due to dependent mechanistic pathways[14]. Thus, to establish a general criterion for effective electrode cleaning, E_2 should be larger than $+600$ mV. However, for $E_2 > +800$ mV, O_2 evolution is excessive and bubble formation can become a problem. Hence, the optimal value $E_2 = +700$ mV is specified. This value corresponds to maximal oxidative cleaning with minimal formation of O_2 bubbles.

The surface oxide formed during application of E_2 in the waveform quickly results in total loss of electrode activity for carbohydrate detection. Hence, the potential step to E_3 gives maximum reactivation of the electrode surface only if all the oxide film is cathodically dissolved during the period t_3. Fig. 8B shows that values of $E_3 << -100$

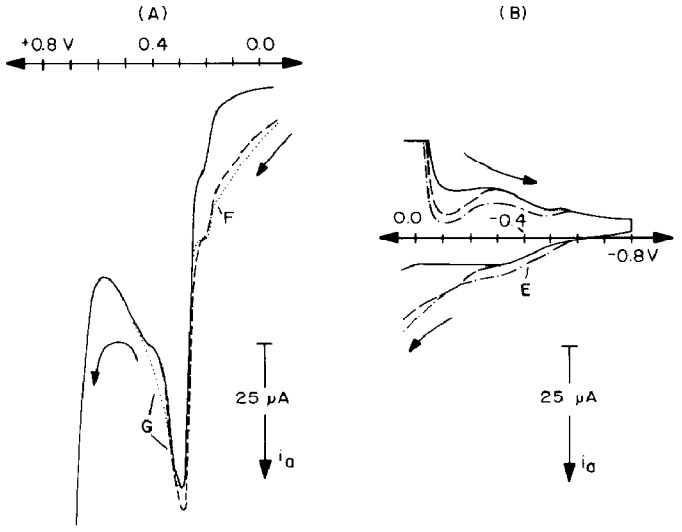

Fig. 8. Comparison of voltammetric responses (i–E) in deaerated 0.1 M NaOH for variation of (A) E_2 and (B) E_3. Only partial positive scans are shown. Conditions and labels: See caption to Fig. 2. Curves: (——) Residual, (-----) 20μM D-fructose, (·····) 20μM sucrose, and (–·–·–) 20μM D-glucose.

mV effectively removes the oxide film generated at E_2. The value $E_3 = -600$ mV, while being sufficient for oxide removal, also avoids any possibility for fouling of the electrode by oxidative reaction of reducing sugars. However, research results indicate virtually no fouling of the Au electrode by oxidation of aldehydes in the region ~ -0.6 to -0.3 V (see Fig. 2, wave E). This observation is indicative of very weak adsorption of the carboxylated detection products which is undoubtedly the result of the hydrophilic nature of this anionic group. Data in Fig. 8B indicate that $E_3 = -300$ mV is sufficient. Other evidence supporting this choice for E_3 is the rise in the background current in Fig. 8B as the potential proceeds from -0.6 to -0.3 V. This wave is attributed to the formation of a partial monolayer of hydrous oxide on the Au surface, *i.e.*, Au–$(H_2O)_{ads.} \rightarrow$ Au–OH + H^+ + e^- (ref. 15). Hence, the step from E_2 to $E_3 = -300$ mV corresponds to the reaction $H^+ + e^-$ AuO $\rightarrow$ Au–OH, and the necessity of reforming this hydrous oxide following the step to E_1 is partially avoided. This results in smaller background signals with the benefit of enhanced stability and reproducibility.

The time periods for application of the oxidative cleaning pulse (t_2) and the cathodic reactivation pulse (t_3) cannot be considered independent of the choices of E_2 and E_3. A larger amount of oxide is formed for a constant t_2 if E_2 is made more positive; hence, a larger t_3 (for constant E_3) or a more negative E_3 (for constant t_3) might be justified to achieve complete oxide removal. The optimization of four interdependent parameters can be exceedingly time consuming. We have determined for $E_2 = +700$ mV that $t_2 = 120$ ms is adequate for oxidative cleaning of Au surface. Chronoamperometric data are shown in Fig. 9 for the process of oxide formation (peak A) during the 120-ms period, following the step from $E_1 = +150$ mV to $E_2 = +700$ mV, and the

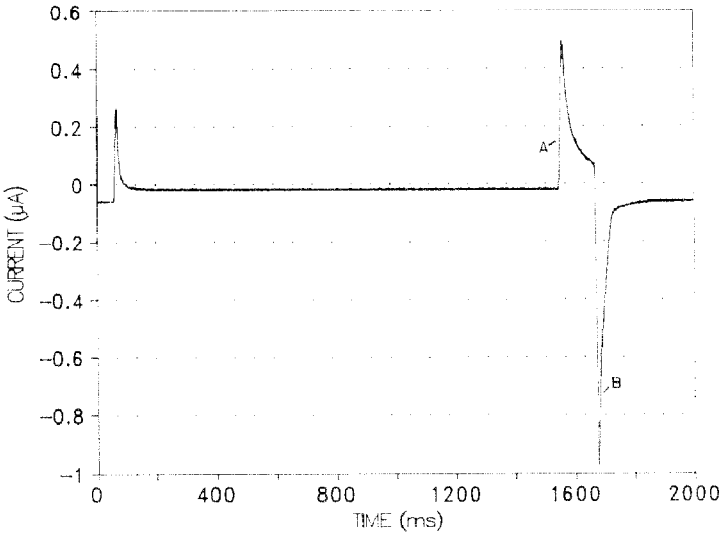

Fig. 9. Chronoamperometric response (i–t) obtained with the optimized p.a.d. waveform (Table 1B, PED) for Au electrode in 0.1M NaOH following the (A) positive and (B) negative potential steps.

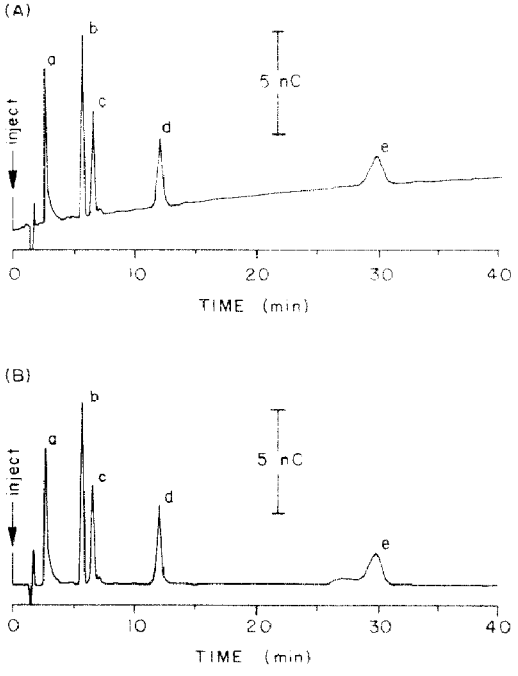

Fig. 10. Comparison of l.c.–p.a.d. results for reactivation periods (t_3) of (A) 120 ms and (B) 360 ms. Conditions and labels: See caption to Fig. 7.

process of cathodic removal of the oxide following the step to $E_3 = -300$ mV (peak B). This data indicates complete removal of the oxide within a 360-ms period. Hence, the optimal value for t_3 is recommended as being $3t_2$. Other research indicates this choice allowed for latitude in the selection of E_2 within the range +600 to +800 mV.

Chromatographic results obtained with $t_2 = 120$ ms are compared in Fig. 10 for $t_3/t_2 = 1$ (curve A) and $t_3/t_2 = 3$ (curve B). Curve A corresponds to an injection made 2 h after initiation of the p.a.d. waveform. The baseline drift in curve A is attributed to the consequence of incomplete oxide reduction for $t_3 = 120$ ms. Curve B corresponds to an injection made only 10 min after initiation of the p.a.d. waveform. Without doubt, the steady baseline in curve B is more desired than that observed in curve A.

With incomplete oxide removal at E_3, a finite rate for continued oxide reduction continues with application of E_1. Hence, a background signal persists which is sensitive to all factors influencing the rate of oxide reduction, *e.g.*, temperature and pH. Another result of inadequate oxide removal is a decreased analytical signal because the electrode surface is not fully utilized for the detection process. These factors have also been noted in the determination of amino alcohols by l.c.–p.a.d.[16]

Effect of pH and organic modifiers. — All carbohydrates that lack a formal charge are weakly acidic with pK_a values in the range of ~ 12–14. Under alkaline conditions, carbohydrates are readily separated in highly efficient anion-exchange columns, and the order of increasing k′ correlates approximately with decreasing values of pK_a for some carbohydrates. Therefore, chromatographic separations are controllable *via* changes in pH, ionic strength, and organic modifiers.

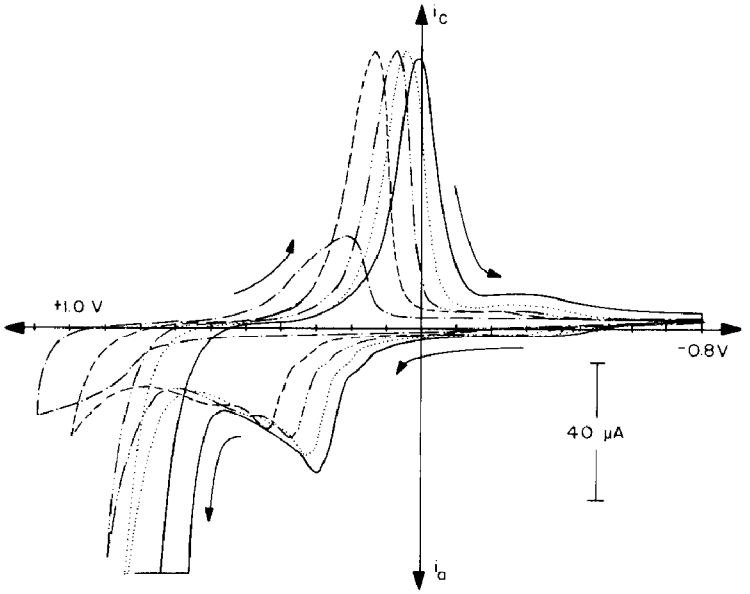

Fig. 11. Effect of pH on voltammetric i–E response of of the Au r.d.e. in 0.1M $NaNO_3$. Conditions: See caption to Fig. 2. Solution pH: (———), pH 14; (·····), pH 13; (–·–·–), pH 12; (-----), pH 11; and (—·—·—), pH 7.

The consideration of pH-gradient elution must recognize the effect of pH change on the background signal as well as the choice of E_1 for maximum sensitivity in l.c.–p.a.d.. The potential for onset of oxide formation at Au electrodes shifts to more negative values with increases in pH at a rate of ~ -60 mV pH^{-1}, as illustrated by the residual i–E curves shown in Fig. 11. These curves are for a Au r.d.e in solutions of 0.1M $NaNO_3$, pH ~7 (— · —); 1mM NaOH/0.1M $NaNO_3$, pH ~11 (——); 10mM NaOH/0.1M $NaNO_3$, pH ~12 (— — —); 0.10M NaOH/0.1M $NaNO_3$, pH ~13 (— · · —); and 1.0M NaOH/0.1M $NaNO_3$, pH ~14 (——). The $NaNO_3$ was added to ensure a high and constant ionic strength. The effect of pH on the oxide formation process is attributable to the pH-dependent nature of Au oxide formation, *i.e.*, $Au(H_2O)_{ads} \rightarrow Au{-}OH + H^+ + e^-$. Because optimal choice of E_1 corresponds approximately to the value for onset of oxide formation, values of E_1 should be adjusted by the amount -60 mV pH^{-1} from the value of +150 mV recommended for 0.1M NaOH.

The negative shift in oxide formation with increasing pH can be reflected by a large baseline change in l.c.–p.a.d. under pH-gradient elution when E_1 remains constant throughout the gradient[17]. This effect can be alleviated to a great extent by substitution of a pH-sensitive glass-membrane electrode for the Ag/AgCl reference electrode in the p.a.d. cell. Because the response of the glass-membrane electrode is ~ -60 mV pH^{-1}, the value of E_1 is automatically adjusted during execution of pH gradients[17].

The linearity of p.a.d. response is relatively unaffected by small changes in pH, as indicated by the data in Table II. The range of linear response for D-glucose by l.c.–p.a.d. is ~10 to 10 000 pmol for mobile phase conditions of 20mM NaOH (pH 12.3), 50mM NaOH (pH 12.7), 100mM NaOH (pH 13), and 200mM NaOH (pH 13.3). Also shown are the linear regression statistics for peak signals in the calibration data. The enhanced sensitivity (increasing slope) with increasing pH is predominantly a result of decreases in k' with increases in pH.

Under ionic strength conditions suitable for electrochemical detection (*i.e.*, $I > 50$ to 100mM), the effect of changing ionic strength is reflected as minor perturbations in the background signal from oxide formation. This effect is not noticed under isocratic l.c. conditions. Under gradient conditions (*e.g.*, increasing acetate concentration), both positive and negative baseline drifts have been observed (data not shown)[17]. Study continues on this phenomenon.

In comparison to ionic strength effects, changes in the concentration of organic modifiers can have a much greater effect on the baseline signal in l.c.–p.a.d.[17]. This can occur, even for electroinactive organic additives, because the modifiers are frequently adsorbed at the electrode surface with a resulting suppression of the oxide formation process. In addition to alteration of the l.c.–p.a.d. baseline, adsorbed organic modifiers can severely attenuate the analytical signal for carbohydrates by interfering with access to specific adsorption sites on the electrode needed for reaction to occur. Weak preadsorption of reacting molecules is considered very beneficial because the residence time of the molecule on the electrode surface is increased substantially, thereby increasing the probability for a successful faradaic reaction.

L.c.–p.a.d. results are shown in Fig. 12 for separation of a carbohydrate mixture

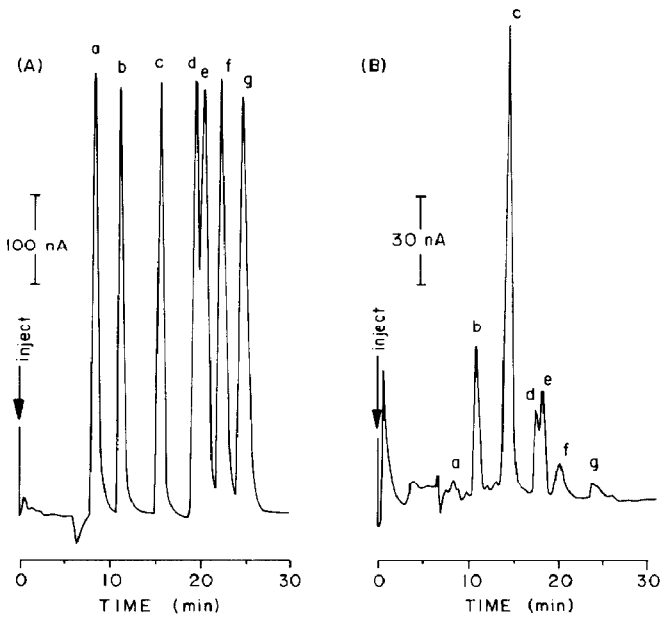

Fig. 12. L.c.–p.a.d. peaks for seven carbohydrates with detection made (A) in the absence and (B) in the presence of 10% acetonitrile added in the mobile phase. Conditions: Column, CarboPac-PA1; mobile phase, 30 mM NaOH at 0.5 mL min^{-1}; post-column reagent at 0.5mL min^{-1}, (A) 0.2M NaOH and (B) 0.2M NaOH/20% acetonitrile; and injection volume, 50 μL. Peaks: (a) D-glucitol, 1.6 nmol; (b) L-fucose, 1.9 nmol; (c) D-galactosamine, 1.5 nmol; (d) D-glucose, 1,9 nmol; (e) *N*-acetyl D-galactosamine, 2.5 nmol; (f) D-fructose, 3.1 nmol; and (g) sucrose, 2.3 nmol.

containing (a) D-glucitol, (b) L-fucose, (c) D-galactosamine, (d) D-glucose, (e) *N*-acetyl-D-galactosamine, (f) D-fructose, and (g) sucrose. Curve A represents the post-column addition of pure 0.1M NaOH, whereas curve B is for post-column addition of 0.2M NaOH/20% acetonitrile. The response for the majority of the sugars is severely attenuated by the presence of the acetonitrile, with a decrease as large as 97% for sucrose. The single exception for this mixture is D-galactosamine whose signal was moderately attenuated by the acetonitrile. The persistence of the signal for D-galactosamine is the beneficial result of the ability of the amine group to adsorb in spite of the presence of acetonitrile on the oxide-free Au surface. In the case of N-acetyl-D-galactosamine, the loss of signal in the presence of acetonitrile is indicative of the weakness (or absence) of amine adsorption as a result of steric hindrance from the acetyl group.

Quantitative parameters. — L.c.–p.a.d. data for separation of five carbohydrates are shown in Fig. 13 to illustrate the response for 100 pmole of each carbohydrate (4μM in each 25-μL injection). The optimum parameters from Table I were used for the p.a.d. waveform. Table III lists the quantitative aspects of the detections on the Au electrode in 0.1M NaOH. Regression analysis of calibration data for these carbohydrates indicates they give linear response from their limit of detection (LOD) up to 1,000 pmoles (40μM). Response above 1,000 pmoles was not tested; however, results from the study of pH effects on linearity (Table II) showed that response for D-glucose was linear to 10 000

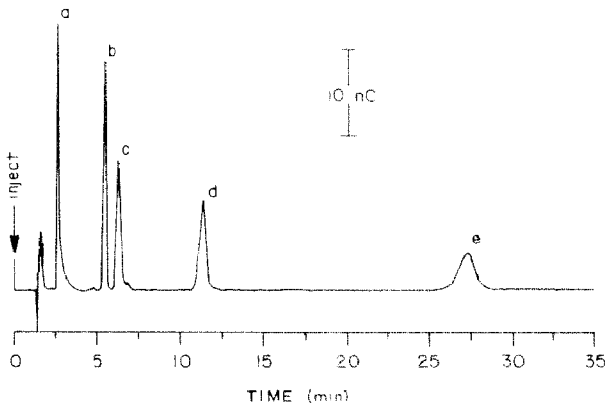

Fig. 13. Chromatogram of several carbohydrates using the optimized PED waveform. Conditions and peaks: See caption to Fig. 6.

TABLE III

Quantitative parameters for five carbohydrates at an Au electrode in 0.1M NaOH[a]

Compound	*Linear range* (pmole – LOD[b])	*Slope* (ncoul./pmole)	*Intercept* (ncoul.)	R^2	*RSD (pmole; n)*
D-glucitol	1000–1	0.249	−1.01	1.0000	12.7 (100; 5)
D-glucose	1000–2	0.247	−0.45	0.9999	3.6 (100; 5)
D-fructose	1000–2	0.137	0.12	1.0000	2.8 (100; 5)
sucrose	1000–2	0.097	0.19	1.0000	2.2 (100; 5)
maltose	1000–5	0.040	0.11	1.0000	1.7 (100; 5)

[a] Carbohydrate response = ncoul. = slope(pmole) + intercept. [b] LOD = limit of detection determined for S:N = 3 from a 5-pmole injection. Average noise is ±0.1 ncoul.

pmoles (400μM) in 0.1M NaOH. The limits of detection range from 1 pmole (40nM, 10 p.p.b.) for D-glucitol to 5 pmole (200nM, 70 p.p.b.) for sucrose. The reproducibility of peak signals for five injections for each carbohydrate range from 1.7 to 3.6% r.s.d. (100 pmole each), except for D-glucitol which had a reproducibility of 12.7% r.s.d. at 100 pmole. The larger %r.s.d. for D-glucitol is attributable to its narrow peak width, which reduces the number of data points (~6–12) describing the D-glucitol peak when using the optimal 2-s waveform. Either increasing the k' or decreasing the cycle time of the waveform is expected to improve the repeatability of early-eluting compounds.

Fig. 14 shows the response of a solution containing 10 pmole of D-glucose in 0.2M NaOH. Values of E_1, E_2, and E_3 are decreased by 20 mV to compensate for the increased alkalinity. Figure 15 is for the assay of a mixture of sugars and amino sugars (10 pmole each) in 0.02M NaOH. Waveform potentials are increased by 40 mV to compensate for the decreased alkalinity. The %r.s.d. for six injections of 10 pmole of L-fucose, D-galactosamine, D-glucosamine, D-galactose, D-glucose, and D-mannose are 7.4, 4.5, 9.3, 3.4, 12.3, and 5.0, respectively.

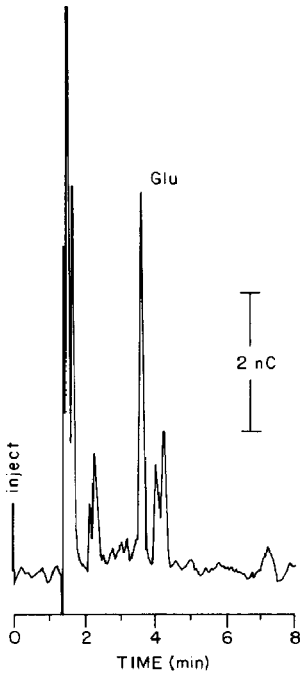

Fig. 14. Chromatogram of 10 pmole of D-glucose. Conditions: Same as Fig. 6, except mobile phase was 0.2M NaOH, and all waveform potentials were reduced by 20 mV.

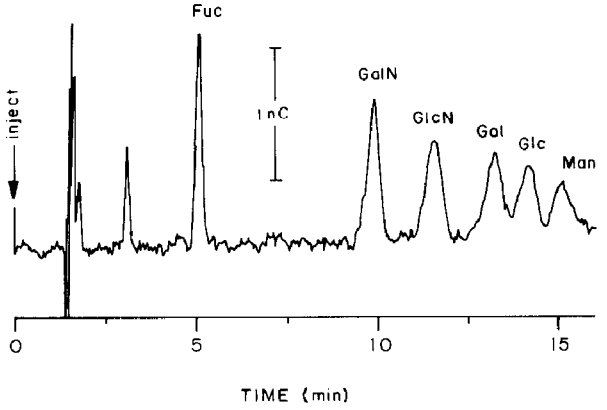

Fig. 15. Chromatographic separation using optimized l.c.–p.a.d. conditions of sample containing 10 pmoles each of L-fucose (Fuc), D-galactosamine (GalN), D-glucosamine (GlcN), D-galactose (Gal), D-glucose (Glc), and D-mannose (Man). Conditions: Same as Fig. 6, except mobile phase was 20mM NaOH, and all waveform potentials were increased by 40 mV.

CONCLUSIONS

The determination of underivatized carbohydrates can be achieved directly and with high sensitivity by anion-exchange chromatography with pulsed amperometric detection (p.a.d.) at Au electrodes in alkaline mobile phases. The guidelines provided in this paper are based upon general principles, and it is expected that they can be applied successfully for virtually all carbohydrates. For some compounds and chromatographic conditions, further optimization of the p.a.d. waveform might be achieved by empirical methods.

ACKNOWLEDGMENTS

The financial support of Dionex Corporation is acknowledged with gratitude.

REFERENCES

1 D. C. Johnson, *Nature*, 321 (1986) 451–452.
2 G. G. Neuburger and D. C. Johnson, *Anal. Chem.*, 59 (1987) 203–204.
3 J. D. Olechno, S. R. Carter, W. T. Edwards, and D. G. Gillen, *Am. Biotech. Lab.*, 5 (1987) 38.
4 D. C. Johnson and W. R. LaCourse, *Anal. Chem.*, 62 (1990) 589A–597A.
5 P. T. Kissinger, in P. T. Kissinger and W. R. Heineman (Eds.), *Laboratory Techniques in Electroanalytical Chemistry*, Marcel Dekker, New York, 1984, pp. 631–32.
6 R. N. Adams *Electrochemistry at Solid Electrodes*, Marcel Dekker, New York, 1969.
7 S. Gilman, in A. J. Bard (Ed.), *Electroanalytical Chemistry*, Vol. 2, Marcel Dekker, New York, 1976, pp. 111–92.
8 B. Fleet and C. J. Little, *J. Chromatogr. Sci.*, 12 (1974) 747–752.
9 H. W. Van Rooijan and H. Poppe, *Anal. Chim. Acta*, 130 (1981) 9–22.
10 R. W. Andrews and R. M. King, *Anal. Chem.*, 62 (1990) 2130–2134.
11 A. J. Bard and L. R. Faulkner *Electrochemical Methods: Fundamentals and Applications*, Wiley, New York, 1980, pp. 283–298.
12 L. A. Larew and D. C. Johnson, *J. Electroanal. Chem.*, 262 (1989) 167–182.
13 W. R. LaCourse, D. C. Johnson, M. A. Rey, and R. W. Slingsby, *Anal. Chem.*, 63 (1991) 134–139.
14 D. C. Johnson, J. A. Polta, T. Z. Polta, G. C. Neuburger, J. Johnson, A. P.-C. Tang, L.-H. Yeo, and J. Bauer, *J. Chem. Soc., Faraday Trans. 1*, 82 (1986) 1081–1098.
15 S. Bruckenstein and M. Shay, *J. Electroanal. Chem.*, 188 (1985) 131–136.
16 W. R. LaCourse, W. A. Jackson, and D. C. Johnson, *Anal. Chem.*, 61 (1989) 2466–2471.
17 W. R. LaCourse, D. A. Mead, Jr., and D. C. Johnson, *Anal. Chem.*, 62 (1990) 220–224.
18 R. R. Townsend and M. R. Hardy, Dionex Corporation, Sunnyvale, CA, personal communication.
19 W. R. LaCourse and D. C. Johnson, in P. Jandik and R. M. Cassidy (Eds.), *Advances in Ion Chromatography*, Vol. 2, Century, Medfield, 1990, pp. 353–372.